σ_A/σ_d at low x and low Q^2*

Stephen Rock and Peter Bosted

University of Massachusetts; Amherst, MA 01003-4525

We have extracted ratios of cross sections for scattering electrons from high mass targets compared to low mass targets in the region of $x \sim 0.02$ and $Q^2 \leq 1$ (GeV/c)^2 from SLAC experiments performed over the past three decades. Additional analysis was needed for radiative corrections, target end caps and calibration runs. We observe no significant difference in the nuclear ratio for low Q^2 compared to results at $Q^2 \geq 1$.

PACS Numbers: 13.60.Hb, 29.25.Ks, 11.50.Li, 13.88.+e

An unexpected strong A, Q^2, x and ϵ dependence of electron-Nucleus inclusive scattering was recently reported by the HERMES collaboration [1] for $x < 0.03$, $Q^2 < 1$ (GeV/c)^2 and $\epsilon < 0.5$. They used the 27 GeV HERA stored polarized electron beam and polarized and unpolarized gas jet targets to measure exclusive and inclusive electron nucleus and nucleon scattering. The observed effect is largest near $x \sim 0.02$ and $Q^2 \sim 0.5$(GeV/c)^2 and $\epsilon \sim 0.5$, where in the lab frame $x = Q^2/(2M\nu)$ is the fractional momentum of the struck quark, Q^2 is the momentum transfer to the scattered electron, ν is the difference between the energy of the incoming and scattered electron, $\epsilon^{-1} = 1 + 2(1+\nu^2/Q^2)\tan^2(\theta/2)$, and θ is the angle of the scattered electron. The EMC effect [2] (the A dependence of the ratio of σ_A/σ_d) had been observed [3] to be almost independent of Q^2 for $Q^2 \geq 1$ (GeV/c)^2 over a large range of Q^2 and x. The HERMES data seem to indicate a large Q^2 dependence of this ratio for $x < 0.03$, $Q^2 < 1$ (GeV/c)^2 and $\epsilon < 0.5$ (dubbed the "HERMES effect"). Miller, Brodsky and Karliner [4] have explained this by coherent contributions from nuclear mesons.

To further explore this kinematic region we have re-examined data from SLAC experiments E61 [5], E140X [6], E154 [7] and E155X. Of these experiments, E61 comes closest to covering the same kinematics as HERMES and uses a wide variety of nuclear targets. The part of the data which is of interest here had not been radiatively corrected due to limitations in computing and theory in the early 1970s. Using more recent radiative corrections programs [8], and the detailed table of materials available in the paper, we have calculated the radiative corrections over the entire measured region. Most targets were 1% radiators. The radiative corrections $\sigma_{Born}/\sigma_{measured}$ are shown in Fig. 1. They are very large at low x and depend strongly on the Atomic Number because of the nuclear elastic tail. Using the Shell Model [9] instead of the Bessel Function Model [10] for the aluminum nuclear elastic cross section would increase the Born cross section by 4% at the lowest x value at 20 GeV and by 2% at 13 GeV. The errors on the Born cross section were calculated using $\delta_{Born} = 1/(\sigma_{meas}/\sigma_{Born} - \sigma_{tail}/\sigma_{Born}) \times \delta_{meas}$ where δ_{meas} is the experimental error on the measured cross section, $\sigma_{tail}/\sigma_{Born}$ is the sum of the nuclear elastic and quasi elastic tails. This results in a very large error for the gold target where these tails are a large fraction of the measured cross section at low x.

Figs 2 and 3 show the E61 Born cross sections for proton and deuteron (per nucleon) compared to the NMC [11] and SMC [12] fits using R1998 [13] for R. The NMC fit is good while the SMC fit is low at low x. Note that these fits did not include data in this kinematic region. The ratio σ_A/σ_d is shown in Tables II and III and Figs. 4 and 5. The solid line is the fit in Gomez *et al.* [14] to data at higher Q^2 corrected for neutron excess. There is excellent agreement between the data and the curves indicating little Q^2 dependence to the A dependence. The lower three x points at $E = 20$ GeV approximately overlap the kinematic region of the HERMES data in x, Q^2 and ϵ. HERMES data are plotted in the panel for aluminum. They are at the same ϵ but slightly higher Q^2. There is a disagreement between the two data sets. The ratio $\sigma_n/\sigma_p = 2 \times \sigma_d/\sigma_p - 1$ is shown in Fig. 6 for the two energies and the last column of Tables II and III. Also shown are the NMC fit [15] to F_2^n/F_2^p and the results from the SMC fit. The NMC fit is in good agreement with the data for most of the data set. The curves may deviate slightly from the data at the lowest values of x at $E = 20$ GeV.

SLAC experiment E140x [6] measured $R = \sigma_L/\sigma_T$ for protons and deuterons. The target assemblies consisted of a cylindrical aluminum cell with thin windows which contained the circulating H_2 or D_2 fluid, as well as an empty cell with thicker windows. We have extracted the ratio of cross sections from the aluminum to deuterium as a function of ϵ to obtain the value of $R_{Al} - R_d$ shown in Table I. At x=0.1 and $Q^2 = 0.5$(GeV/c)^2, the average ratio of cross sections is 1.02 $\pm$ 0.007 and is independent of ϵ resulting in $R_{Al} - R_d$ = -0.033 $\pm$ 0.052, $R_{Al}/R_d = 0.9 \pm 0.2$. Comparison with the value of $R_N/R_d \sim 5$ reported by HERMES at $x \leq 0.03$ and the same Q^2 would require a very rapid increase in R as a function of x.

*Work supported by the National Science Foundation and the Department of Energy.

The calibration data from E154 was used to determine the ratio $\sigma_{glass}/\sigma_{^3He}$ in the kinematic range $x \geq 0.017$ and $Q^2 \geq 1.5(\mathrm{GeV/c})^2$ for $\epsilon \geq 0.4$. This borders on the region where HERMES sees a large deviation from the EMC effect for the ratio of cross sections for nitrogen to ^3He. The average A for the glass used is ~ 21 compared to $A = 14$ for Nitrogen. The EMC effect depends logarithmically on A and if the HERMES effect does the same, there would be an enhancement in the effect of about 15% of its value. The experiment [7] was designed to measure g_1 and g_2 for the neutron. The polarized target was ^3He at 10 atmospheres pressure inside a glass cylinder. The cylinder end caps and gas were of similar areal density. There was also a calibration cell of almost identical design except that the gas pressure could be varied. Only ratios of counting rates were measured since the acceptance of the spectrometer is not known to sufficient accuracy to determine useful absolute cross sections. All rates were corrected for dead time and pion contamination. The dead time was both rate and x dependent, with a maximum of about 10% at low x for a full target. An estimated uncertainty of 30% in the dead time correction corresponds to about 4% systematic error on the counting rate ratios. The counting rate from helium was determined by fitting the total counting rate as a function of the pressure in the calibration cell. The counting rate from glass was found by subtracting the pressure-normalized ^{3}He counting rate from the counting rate of the corresponding polarized cell. Four different calibration cells and 9 different polarized cells were used. The ratio $\sigma_{glass}/\sigma_{^3He}$ was determined from the ratio of counting rates and the measured dimensions of the polarized target, the helium density, the chemical composition of the glass, a fit to the ratio σ_n/σ_p [15], and radiative corrections. The measurements on the 9 targets scatter about the average with an width of less than 1 sigma. indicating that some of the errors, like radiative corrections, are correlated between targets. Fig. 7 show $\sigma_{glass}/\sigma_{^3He}$ averaged over all the measurements as a function of x as measured by the spectrometers located at 2.75^o and 5.5^o. The errors are statistical plus systematic. The results are consistent with a fit to the EMC effect [14], except perhaps at the large x at 2.75^o. Our lowest x point is at $x = .017$, $Q^2 = 1.5(\mathrm{GeV/c})^2$ and $\epsilon = .37$. The closest HERMES points (open squares) are at similar x and ϵ, but $Q^2 < 1(\mathrm{GeV/c})^2$ and have a systematic error of ~ 0.03. Within this systematic error E154 does not exclude the HERMES results within the region of overlap.

Experiment E155X used a NH_3 cryogenic polarized target to measure the polarized structure function g_2. The beam energies of 29 and 32 GeV were approximately the same as HERMES. The spectrometers at 2.75^o and 5.5^o measured the scattered electrons. A carbon target was also used for calibration. From the ratio of the counting rates on carbon and NH_3, we were able to determine the ratio σ_C/σ_d. The method assumed that the cross sections for all the materials in the targets (1.72 gms NH_3, 0.22 gms ^{4}He, 0.184 gms Al and 0.016 gms Cu or 1.51 gms C, 0.39 gms ^{4}He, and 0.18 gms Al) scaled in A by the relative EMC effect [14]. The ratio was normalized to the predicted ratio using the data from the 2.75^o spectrometer for $x \geq 0.15$ and from the 5.5^o spectrometer. The x dependent systematic errors come from radiative corrections, tracking efficiency, the mass of the Cu NMR coil in the NH_3 target and the uncertainty in σ_p/σ_d. Because of the small fraction of Hydrogen in the polarized target, the error on σ_C/σ_d is approximately 6 times the error on σ_{NH_3}/σ_C, leading to a systematic error of about 10%. Figs. 8a and b show the ϵ and Q^2 values for the beam energies of 29 GeV(dashed curve) and 32 GeV (solid curve) as a function of x. Unfortunately the data do not extend down to $x \leq 0.02$ where the HERMES effect is largest. Fig. 8c and d show the 29 and 32 GeV cross section ratios as the solid circles. The curve is the EMC effect [14] and the open squares are the approximate values of the HERMES effect [1] taken from their plots. The E155X data agree both with the EMC effect curve and with the HERMES points within the 10% systematic errors.

In conclusion, SLAC data from several experiments are consistent with the previously parameterized EMC effect and constrain the possibility of large effects as seen by HERMES. Experiment E61 used different target at the same kinematics. E155X had similar kinematics, but large systematic errors. Experiments E140X and E154 used different high mass targets at nearby kinematics. Thus none of the experiments directly contradicts the HERMES results on σ_N/σ_d. However a smooth interpolation between targets in E61 does not support the HERMES result.

---

[1] HERMES collaboration, K. Ackerstaff *et al.* hep-ex/9910071.
[2] EMC Collaboration, J. J. Aubert *et al.*, Phys. Lett. B123 (1983) 275.
[3] NMC Collaboration, P. Amaudruz *et al.* Nucl. Phys. B441 (1995) 3, hep-ph/9503291; M. Arneodo *et al.* Nucl. Phys. B441 (1995) 12,hep-ex/9504002.
[4] G. A. Miller, S. J. Brodsky and M. Karliner, hep-ph/0002156.
[5] S. Stein *et al.*, Phys. Rev. D12 (1975) 1884.
[6] SLAC E140x, L.H. Tao *et al.,* Z. Phys. C70 (1996) 387.

[7] E154 Collaboration, K. Abe *et al.*, Phys. Rev. Lett. **79**, 26 (1997),ep-ex/9705012.
[8] SLAC E140, S. Dasu *et al.,* Phys. Rev. Lett. 61, 1061 (1988) and references within.
[9] S. Stein *et al.,* Phys. Rev. D12 (1975) 1884.
[10] H. de Vries, C. W. de Jager, and C. de Vries, Atomic Data and Nuclear Data Tables 36 (1987) 495.
[11] NMC Collaboration, M. Arneodo *et al.,* Phys. Lett. B364 (1995) 107,hep-ph/9509406 .
[12] SMC Collaboration, Phys. Rev. D58 (1998) 112001.
[13] J. Fellbaum *et al.* Phys. Lett. B452 (1999) 194, hep-ex/9808028.
[14] J. Gomez *et al.,* Phys. Rev. D49, 4348 (1994).
[15] P. Amaudruz *et al.,* Nucl. Phys. B371 (1992) 3.

TABLE I. $R_{Al} - R_d$ and R_{Al}/R_d

x	Q^2	$R_{Al} - R_d$	R_{Al}/R_d	χ^2/df
0.10	0.5	-0.033 ± .053	0.87 ± .20	0.5
0.10	1.0	0.055 ± .118	1.16 ± .34	0.4
0.35	3.0	0.074 ± .107	1.33 ± .46	0.8
0.50	3.6	-0.011 ± .083	0.94 ± .43	4.5

TABLE II. Ratio of Born cross sections for E=13 GeV

x	Q^2	ϵ	Be/d	Al/d	Cu/d	Au/d	σ_n/σ_p
0.182	0.69	0.98	0.99±0.02	1.00±0.02	1.03±0.02	0.99±0.04	0.84±0.03
0.136	0.66	0.97	1.01±0.02	1.02±0.02	1.06±0.02	1.05±0.03	0.82±0.03
0.104	0.62	0.96	1.03±0.02	1.01±0.02	1.07±0.02	1.08±0.04	0.85±0.03
0.080	0.58	0.94	0.99±0.01	1.00±0.01	0.99±0.02	1.04±0.03	0.86±0.02
0.061	0.53	0.91	1.00±0.02	0.99±0.01	0.98±0.02	0.99±0.03	0.87±0.02
0.047	0.48	0.87	0.99±0.02	0.97±0.01	0.96±0.02	1.04±0.04	0.85±0.02
0.036	0.43	0.81	0.97±0.02	0.95±0.02	0.95±0.02	0.95±0.03	0.89±0.03
0.027	0.37	0.74	1.03±0.03	0.95±0.03	0.94±0.03	0.92±0.04	0.85±0.04
0.020	0.30	0.65	0.96±0.03	0.91±0.03	0.90±0.04	0.84±0.05	0.94±0.06

TABLE III. Ratio of Born cross sections for E=20 GeV

x	Q^2	ϵ	Be/d	Al/d	Cu/d	Au/d	σ_n/σ_p
0.228	1.59	0.98	0.99±0.02	1.02±0.02	1.04±0.02	0.97±0.04	0.72±0.02
0.186	1.52	0.97	1.00±0.02	1.05±0.01	1.06±0.03	1.04±0.04	0.76±0.02
0.152	1.45	0.96	1.02±0.02	1.02±0.02	1.03±0.02	1.05±0.03	0.81±0.02
0.124	1.37	0.94	1.02±0.02	1.06±0.02	1.09±0.03	1.12±0.05	0.81±0.02
0.102	1.29	0.92	1.01±0.02	1.02±0.02	1.04±0.02	1.05±0.03	0.83±0.02
0.084	1.20	0.89	0.99±0.02	1.03±0.02	1.06±0.03	1.04±0.04	0.86±0.02
0.068	1.11	0.86	1.01±0.01	0.99±0.02	1.03±0.02	1.05±0.03	0.82±0.02
0.055	1.00	0.81	0.97±0.02	1.00±0.02	1.05±0.04	1.11±0.05	0.87±0.03
0.044	0.90	0.76	0.97±0.02	0.97±0.02	0.95±0.02	0.89±0.03	0.89±0.02
0.035	0.78	0.69	0.98±0.02	0.95±0.02	-	0.94±0.05	0.89±0.02
0.027	0.66	0.61	0.98±0.03	0.91±0.02	0.90±0.04	0.81±0.06	0.86±0.03
0.020	0.54	0.51	0.99±0.03	0.89±0.03	0.85±0.05	0.87±0.08	1.03±0.04
0.014	0.40	0.40	0.99±0.05	0.87±0.04	0.86±0.08	0.82±0.14	1.04±0.07

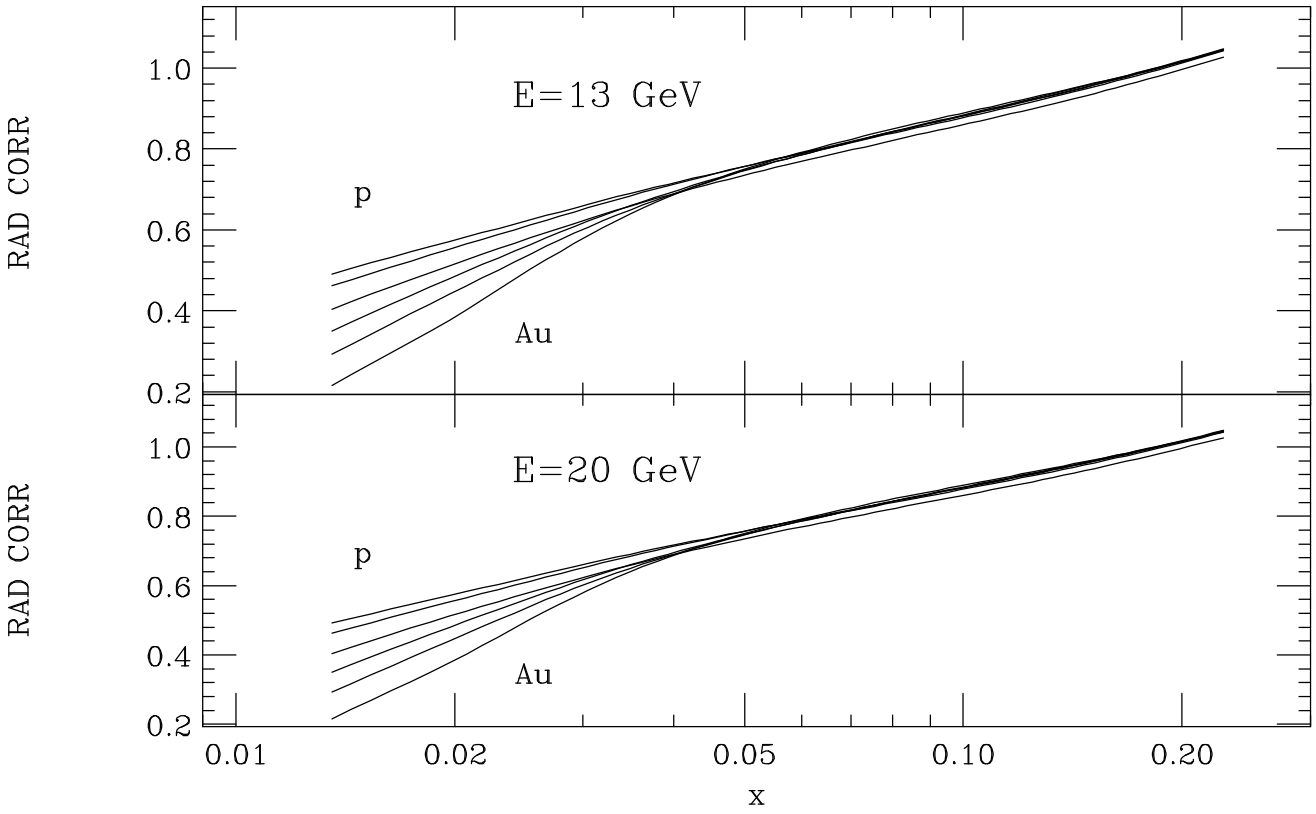

FIG. 1. Radiative Corrections for proton, deuteron, Be, Al, Cu and Au for two different beam energies vs. x. At low x the corrections are large and different for the different materials due to the nuclear elastic tail. The labels 'p' and 'Au' indicate which curves correspond to which nuclei (changing monotonically).

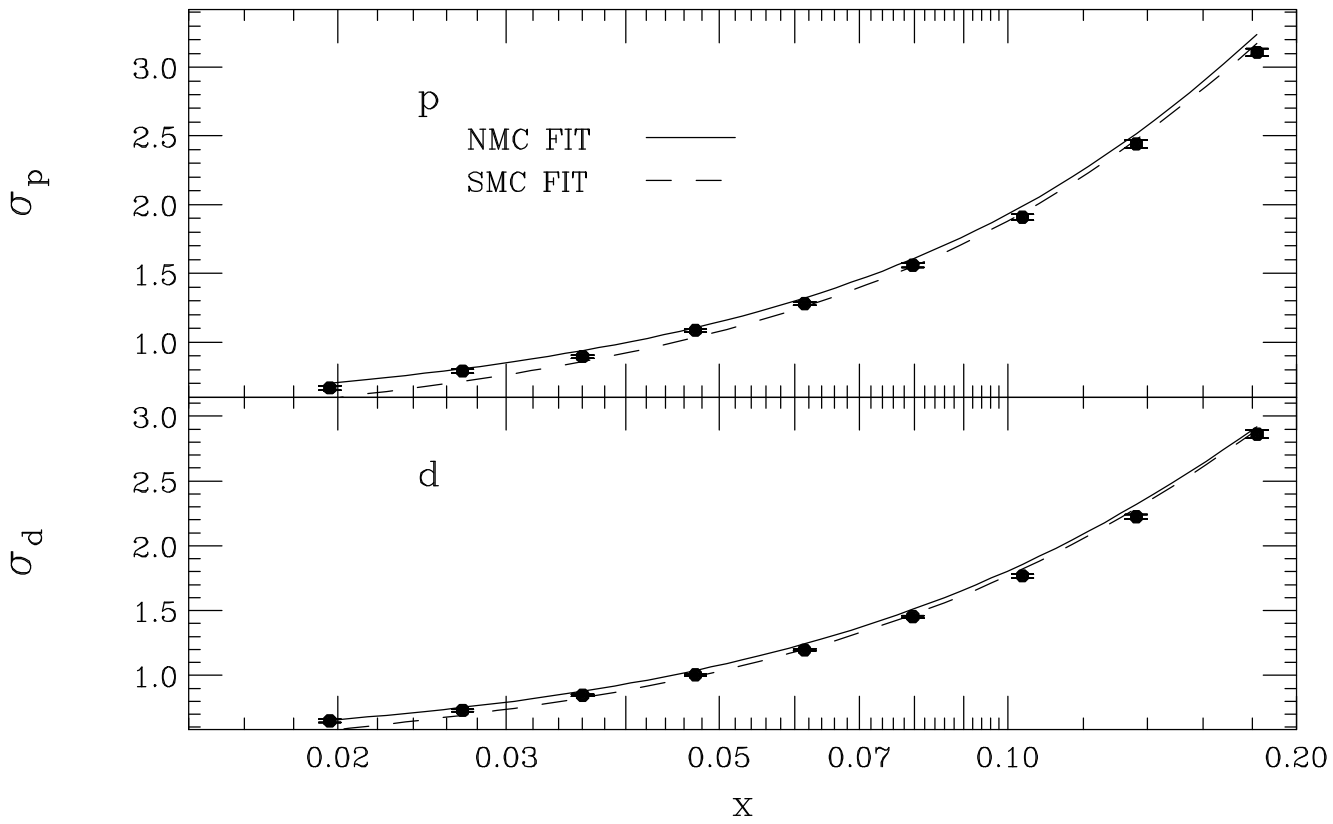

FIG. 2. Born cross sections for proton and deuteron (per nucleon) at 13 GeV from Stein et al. compared to the NMC (solid) and SMC (dash) fit. These fits did not include data in this region. The NMC fit is good, while the SMC fit is low at low x.

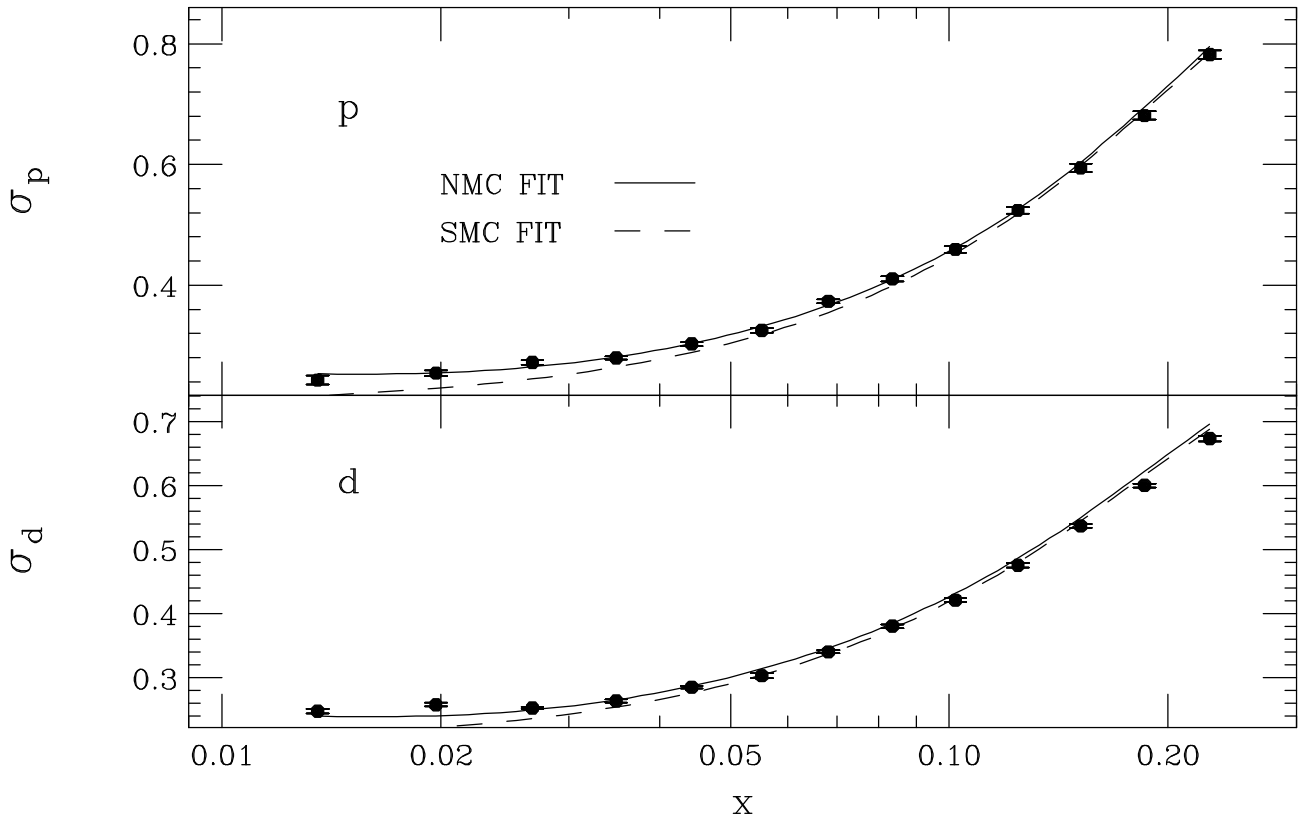

FIG. 3. Born cross sections for proton and deuteron (per nucleon) at E=20 GeV. from Stein et al. at 20 GeV compared to the NMC (solid) and SMC (dash) fit. These fits did not include data in this region. The NMC fit is good, while the SMC fit is low at low x.

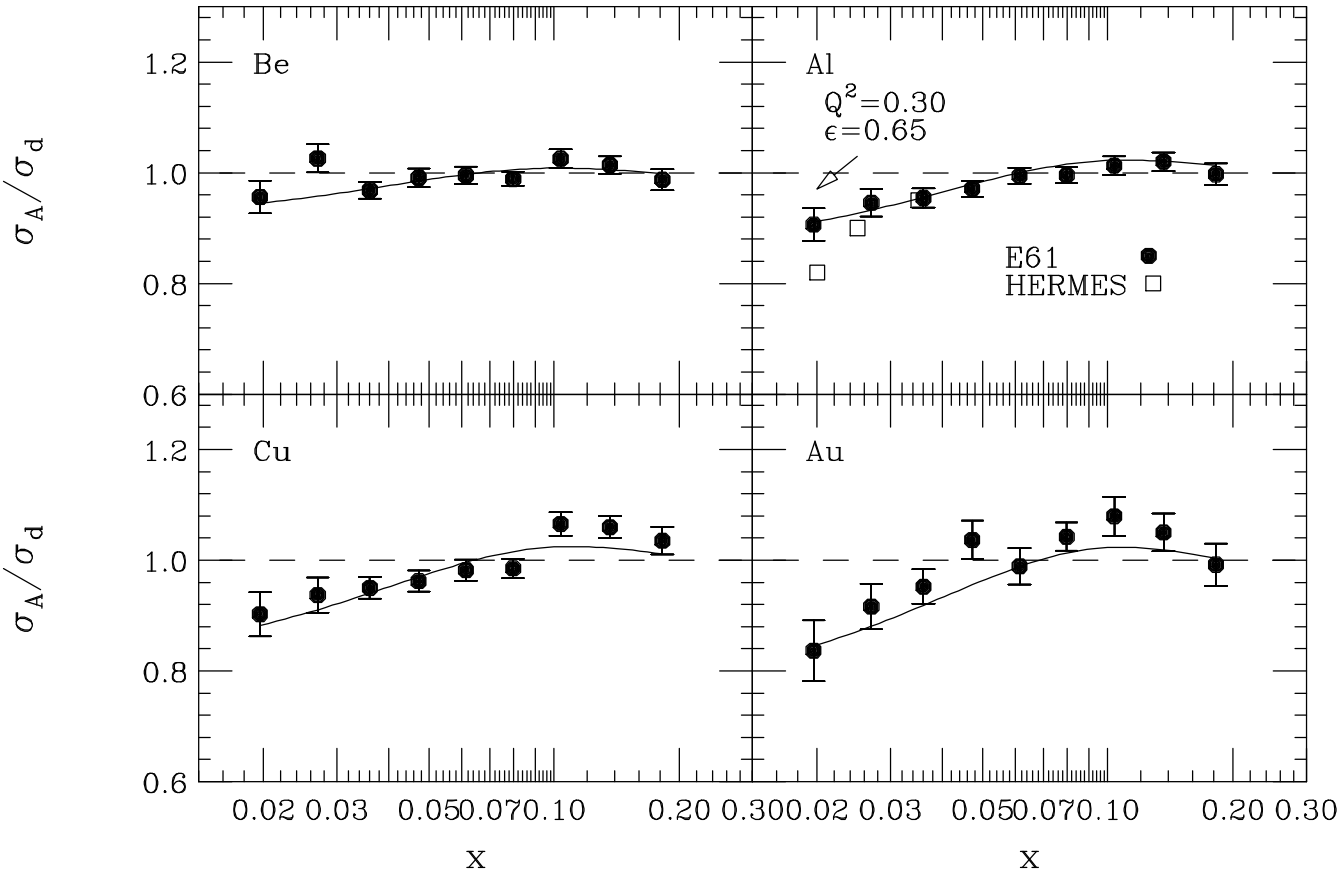

FIG. 4. σ_A/σ_d as a function of x for E=13 GeV. The lowest x points have $(Q^2, \epsilon) = (0.3,0.65)$, $(0.37,0.74)$. The curve is the fit [14] to EMC effect data at $Q^2 > 1(\mathrm{GeV/c})^2$. Also shown with the aluminum results are the HERMES data [1] for σ_N/σ_d at the same ϵ. The HERMES systematic error is ~ 0.03.

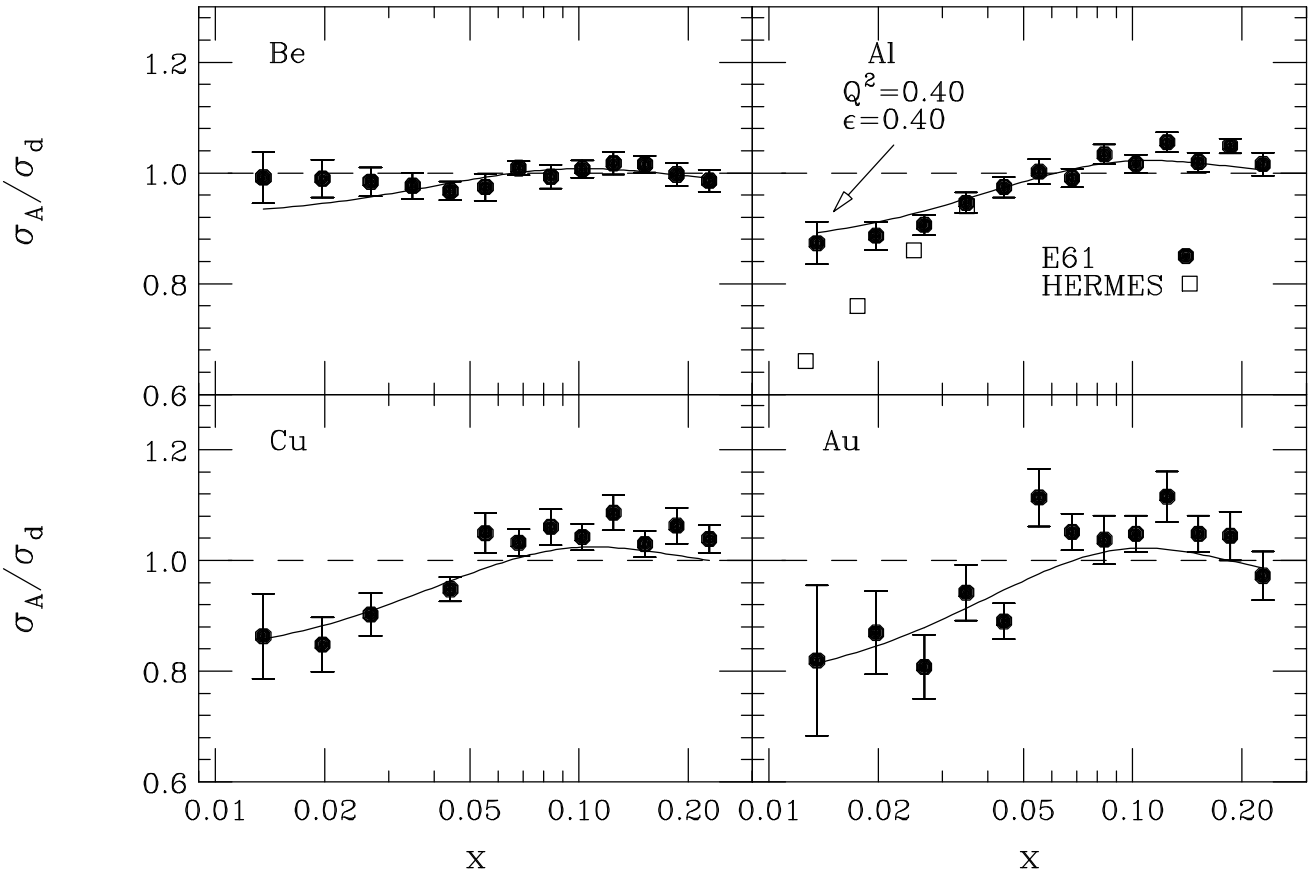

FIG. 5. σ_A/σ_d as a function of x for E=20 GeV. The lowest x points have (Q^2, ϵ) =(0.40,0.40), (0.54,0.51), (0.66, 0.61.) which overlap in x and ϵ some of the HERMES data shown as open squares. The HERMES systematic error is ~ 0.03. The curve is the fit [14] to EMC effect data at $Q^2 > 1(\mathrm{GeV/c})^2$.

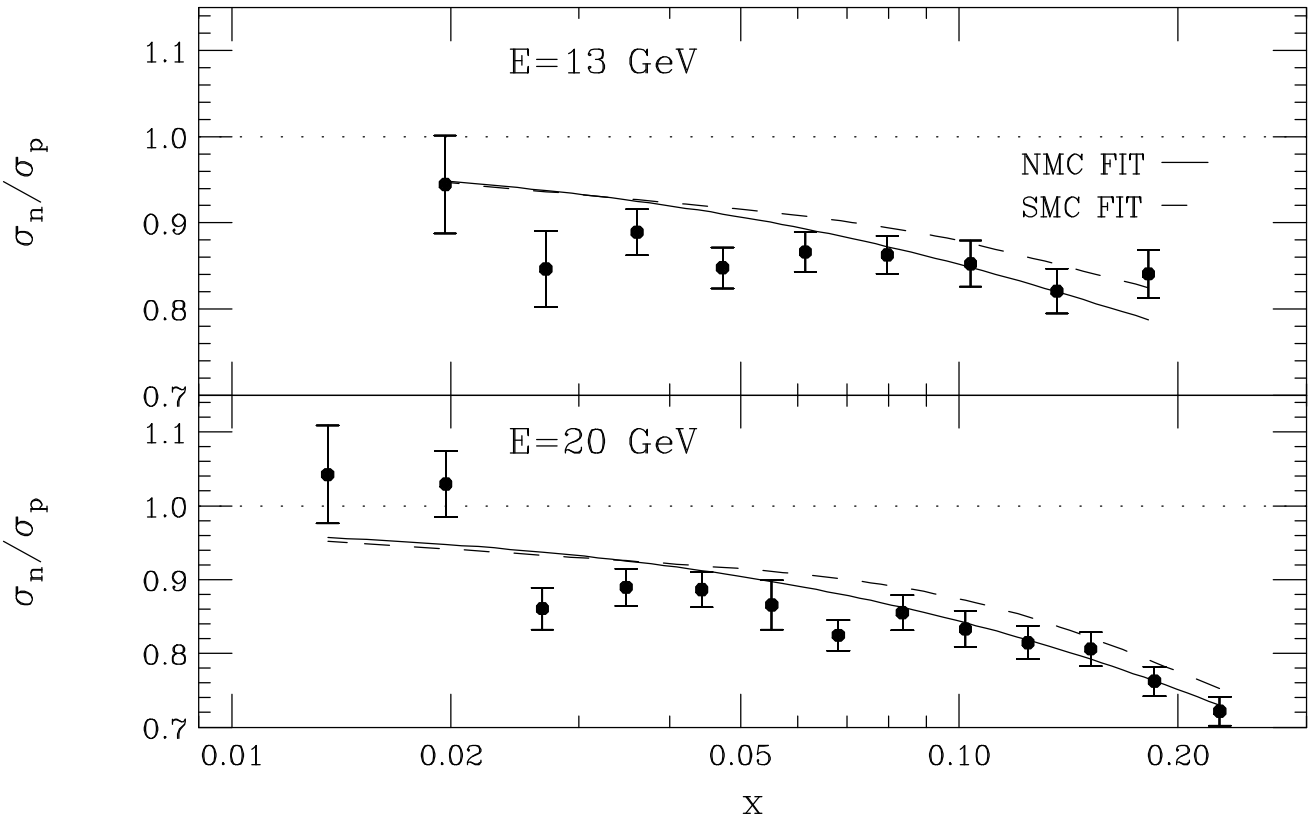

FIG. 6. σ_n/σ_p as a function of x for E=13 and 20 GeV. Also shown are the NMC and SMC fits to F_2^n/F_2^p.

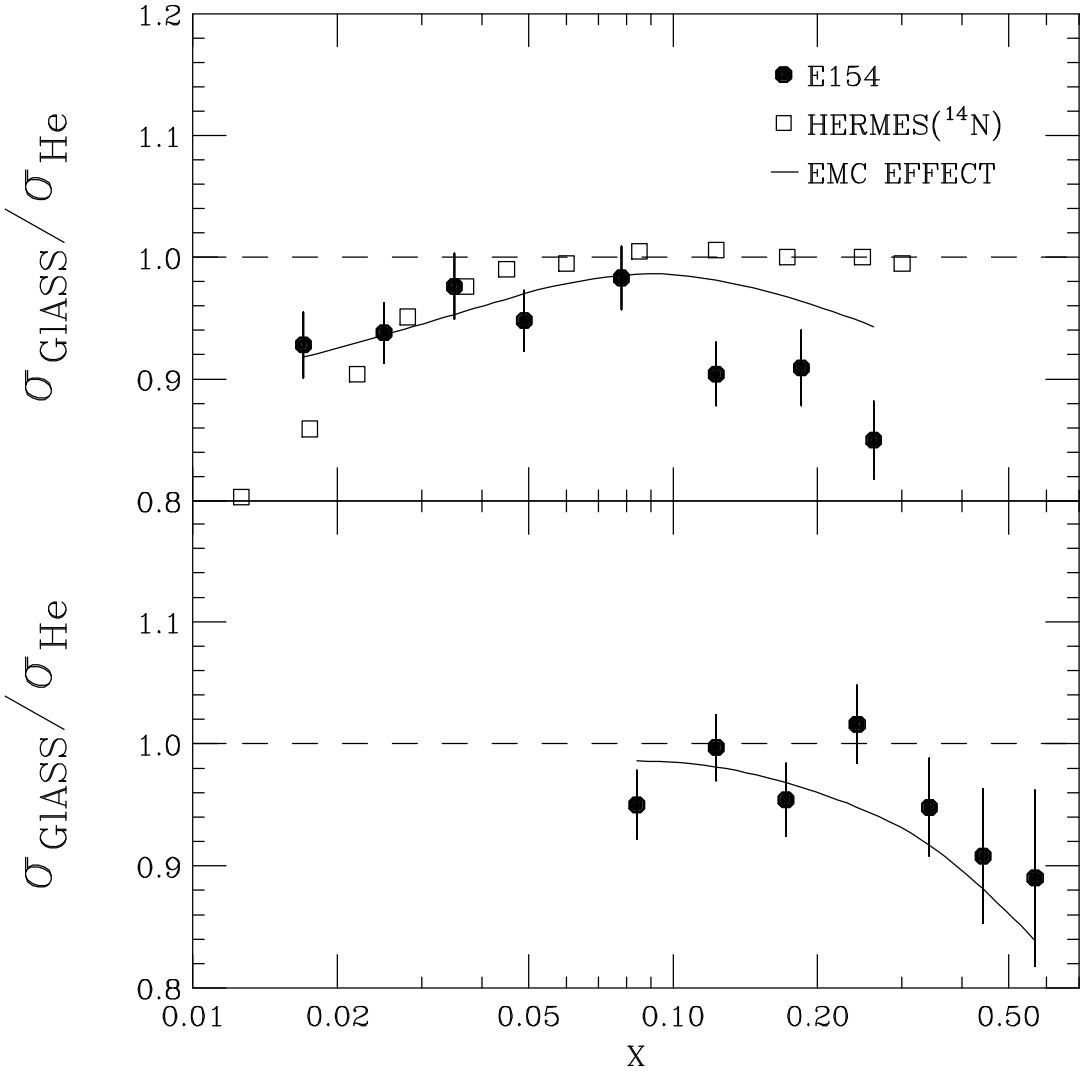

FIG. 7. Measured ratio of cross sections glass/^{3}He at top) 2.75^o and bottom) 5.5^o. The E154 results (solid circle) are at $Q^2 > 1(\mathrm{GeV/c})^2$. The errors are the total errors. The three lowest HERMES [1] points (open squares) are at $Q^2 < 1$ $(\mathrm{GeV/c})^2$. The HERMES systematic error is ~ 0.03 The solid curve is a fit to the EMC effect [14].

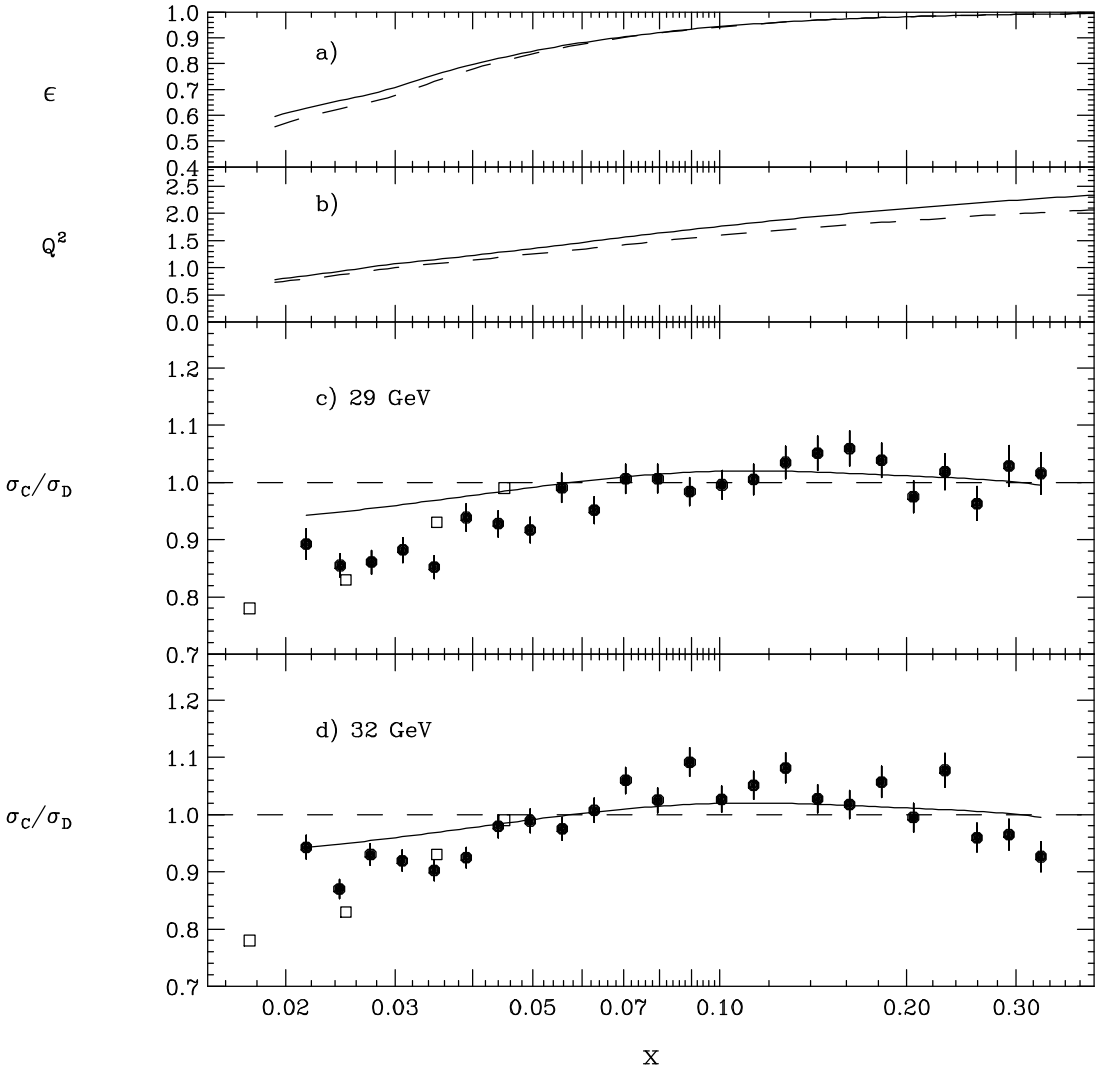

FIG. 8. Results from Experiment E155X on the Ratio σ_C/σ_d. a,b) ϵ and Q^2 as a function of x for the beam energies of 29 (dash) and 32 (solid) GeV. c,d) The ratio σ_C/σ_d from E155x (solid circles), and from HERMES (open squares) [1]. There is a 10% systematic error on the E155x results. The solid curve is a fit to the EMC effect at higher value of Q^2.